

Pressure-stabilized Li_2K electride with superconducting behavior

Xiao-Zhen Yan(颜小珍), Quan-Xian Wu(邬泉县), Lei-Lei Zhang(张雷雷), and Yang-Mei Chen(陈杨梅)
Citatio: Chin. Phys. B, 2025, 34 (**9**): 097405. DOI: 10.1088/1674-1056/add009
http://cpb.iphy.ac.cn; http://iopscience.iop.org/cpb

What follows is a list of articles you may be interested in

Superconductivity and band topology of double-layer honeycomb structure M_2N_2 (M = Nb, Ta)

Jin-Han Tan(谭锦函), Na Jiao(焦娜), Meng-Meng Zheng(郑萌萌), Ping Zhang(张平), and Hong-Yan Lu(路洪艳)
Chin. Phys. B, 2025, 34 (**9**): 097402. DOI: 10.1088/1674-1056/adee04

Surface reconstruction modulated superconductivity on quasi-2D iron pnictide superconductor $KCa_2Fe_4As_4F_2$

Wenjing Zeng(曾文静), Zongyuan Zhang(张宗源), Xiaoyan Dong(董晓燕), Yubing Tu(涂玉兵), Yanwei Wu(吴彦玮), Teng Wang(王腾), Fan Zhang(张凡), Shuai Shao(邵帅), Jie Hou(侯杰), Xingyuan Hou(侯兴元), Ning Hao(郝宁), Gang Mu(牟刚), and Lei Shan(单磊)
Chin. Phys. B, 2025, 34 (**8**): 087402. DOI: 10.1088/1674-1056/add5cb

Superconductivity in YbN_4H_{12} under low pressures

Xiang Wang(汪翔), Chenlong Xie(谢晨龙), Haohao Hong(洪浩豪), Yanliang Wei(魏衍亮), Zhao Liu(刘召), and Tian Cui(崔田)
Chin. Phys. B, 2025, 34 (**8**): 087401. DOI: 10.1088/1674-1056/add908

Theoretical investigation of potential superconductivity in Sr-doped $La_3Ni_2O_7$ at ambient pressure

Lei Shi(石磊), Ying Luo(罗颖), Wei Wu(吴为), and Yunwei Zhang(张云蔚)
Chin. Phys. B, 2025, 34 (**7**): 077403. DOI: 10.1088/1674-1056/add1bd

Fabrication and characterization of MgB_2 spherical shells with reduced thickness on 1 mm diameter Si_3N_4 spheres

Ruining Sun(孙瑞宁), Tiequan Xu(徐铁权), Yue Wang(王越), Furen Wang(王福仁), and Zizhao Gan(甘子钊)
Chin. Phys. B, 2025, 34 (**7**): 077402. DOI: 10.1088/1674-1056/adcdec

---

Pressure-stabilized Li_2K electride with superconducting behavior

Xiao-Zhen Yan(颜小珍)[1], Quan-Xian Wu(邬泉县)[1], Lei-Lei Zhang(张雷雷)[2], and Yang-Mei Chen(陈杨梅)[1,†]

[1] *School of Science, Jiangxi Provincial Key Laboratory of Particle Technology, Jiangxi University of Science and Technology, Jiangxi* 341000, *China*
[2] *Institute of Nano-Structured Functional Materials, Huanghe Science and Technology College, Zhengzhou* 450063, *China*

(Received 4 February 2025; revised manuscript received 20 April 2025; accepted manuscript online 24 April 2025)

Compression of alkali elements makes them depart gradually from the s-band metals, leading to exotic physical and chemical properties. Here, we report the chemical reaction $Li + K \rightarrow Li_2K$ under high pressure by using a swarm intelligence structure searching methodology combined with first-principles calculations. Li_2K has three stable/metastable structures and undergoes the pressure-induced phase transitions $C2/m \rightarrow Fddd \rightarrow I4/mmm$ at 226 GPa and 291 GPa, respectively. Notably, this system features significant s $\rightarrow$ p and s $\rightarrow$ d charge transfers as well as a topologically zero-dimensional electride character. Under 300 GPa, Li_2K manifests exceptional superconductivity with a critical temperature (T_c) of 39 K, attributed to the orbital hybridization between Li p states and interstitial quasi-atom-derived s electrons, and their robust coupling with Li and K phonon modes. This work serves as a crucial reference for exploring novel superconducting electrides.

Keywords: superconductivity, high pressure, first-principles study, electride

PACS: 74.70.–b, 62.50.–p, 63.20.dk, 87.15.Zg

DOI: 10.1088/1674-1056/add009 **CSTR:** 32038.14.CPB.add009

1. Introduction

Alkali metals, characterized by their single valence electron and simple electronic structure, have long served as prototypical systems for understanding fundamental metal physics. At ambient pressure, these elements adopt body-centered cubic (bcc) structures and exhibit "free-electron-like" behavior, consistent with textbook descriptions of metals. However, under high pressure, their properties undergo a dramatic transformation[1–15] such as improved superconductivity[16–18] and counterintuitive chemistry.[19–28] For example, metastable LiCs alloy forms at ultra-low pressures (0.1 GPa) due to the large difference in electronegativity between Li and Cs.[29] Theoretical calculations indicate that Cs becomes more electronegative than Li under extreme pressure, driving the formation of stable Li-rich phases (Li_nCs) with critical temperature (T_c) up to 54 K.[26,27] LiNa stabilizes in an insulating compound with a 3.67 eV bandgap at 355 GPa.[24] Na–K alloys exhibit complex pressure-dependent behavior: Na_2K is stable at ambient pressure and undergoes decomposition–recombination at 10–500 GPa.[22] Three additional ground-state phases (NaK, NaK_3, Na_3K_2) and a potentially superconducting NaK_2 phase emerge, with T_cs of 12.17 K and 6.26 K at 250 GPa and 400 GPa, respectively.[20,30]

In recent years, Li-based electrides have emerged as a particularly compelling class of materials, showcasing remarkable superconducting properties and providing new insights into superconducting mechanisms.[31–42] For instance, at 270 GPa Li_6P demonstrates a T_c of 39.3 K in its proposed *R*-3*m* phase, characterized by a p-orbital-dominated electronic state.[34] This state plays a pivotal role in softening acoustic phonons and forming itinerant hybridized p-orbital electronic states, thereby enhancing electron–phonon (e–p) coupling and facilitating high-temperature superconductivity. Li_6C exhibits superconductivity under relatively mild pressures, achieving a T_c of 10 K at 80 GPa.[42] This high T_c is primarily attributed to the synergistic effects of interatomic coupling, phonon softening and the cooperative action of phonon-coupling bands, which are predominantly governed by host sp-hybridized electrons rather than interstitial quasi-atoms (ISQs). The sp-hybridized cage-like ISQs serve as a chemical precompression mechanism, reducing the required dynamic stabilization pressure. Li_8Au stands out with a record-breaking T_c of 73.1 K at 250 GPa, attributed to its unique NaCl-type (B1) lattice featuring octahedrally coordinated interstitial Au electrons at the center of cubic Li_8 cages. The robust e–p coupling in Li_8Au is primarily driven by the coupling between interstitial Au electrons and medium-frequency vibrations, contributing to its exceptional superconducting performance. Li_6La has a T_c of 16.3 K at 200 GPa, originating from enhanced coupling between ISQs and low-frequency phonons.[33] Additionally, this compound undergoes a superionic phase transition at high temperatures, highlighting the coexistence of superconductivity and superionicity. In $Li_{10}Si$, superconductivity with a T_c of 14.7 K at 95 GPa is reinforced by the coupling between Li p electrons and low-frequency Li-dominated phonon softening.[43] Notably, this material also exhibits a superionic

†Corresponding author. E-mail: chenyangmei@jxust.edu.cn

© 2025 Chinese Physical Society and IOP Publishing Ltd. All rights, including for text and data mining, AI training, and similar technologies, are reserved.

state at 60 GPa and 850 K, where Si atoms form a rigid lattice while Li ions freely diffuse.

These findings offer valuable insights into designing novel electride superconductors. In this paper, we perform a first-principles study on the phase stability, electronic and superconducting properties of Li_2K under high pressures.

2. Computational methods and details

We perform structure searches for Li_2K at 100 GPa, 300 GPa, 500 GPa and 700 GPa with one to four formula units per cell using the CALYPSO (Crystal structure AnaLYsis by Particle Swarm Optimization) code, which is efficient at predicting structures of materials.[44–47] Structural relaxations and electronic structure calculations are carried out using the Vienna *ab initio* simulation package[48] with the local density approximation in the framework of density functional theory.[49,50] We use projector-augmented-wave pseudopotentials[51] in which $1s^2 2s^1$ and $3s^2 3p^6 4s^1$ are treated as valence electrons for Li and K. The cut-off energy is set to 650 eV in these calculations, and the Monkhorst–Pack grid with a maximum spacing of 0.02 $Å^{-1}$ is individually adjusted in reciprocal space to the size of each computational cell, which usually gives total energies converged to ~ 1 meV per atom. The phonon dispersion curves and the e–p coupling are computed using the density functional perturbation theory as implemented in the Quantum ESPRESSO code.[52] The formation enthalpy (ΔH) of Li_2K with respect to elemental Li and K is calculated using the formula $\Delta H(Li_2K) = [H(Li_2K) - 2H(Li) - H(K)]/3$, where H is the enthalpy of the most stable structure of certain compositions at the given pressure, For Li, *Cmca*-24, *Cmca*-56, $p4_2/mbc$ and $Fd\bar{3}m$ are adopted,[2,53,54] and for K, *Cmca* and *hP*4 are adopted.[2,3,55]

3. Results and discussion

The crystal structure plays a critical role in determining the physical properties of materials. We first perform systematic searching simulations of crystal structures of Li_2K at 100 GPa, 300 GPa, 500 GPa and 700 GPa. The predicted stable structures are presented in Fig. 1. At 100 GPa, a monoclinic structure with $C2/m$ symmetry is found to have the lowest enthalpy. In this phase, both the Li and K atoms arrange in layers of sheets. At 300 GPa, we find two possible packings that are energetically competitive, one in the $Fddd$ symmetry and the other in $I4/mmm$. The former is ~ 2 meV/atom lower in energy than the latter. In the $Fddd$ phase, the nearest Li atoms braid together and interlace to form a network sublattice with the K atoms embedded within. In the $I4/mmm$ phase, the Li atoms form a cage-like sublattice with the K atoms surrounded in the centers.

To determine the thermodynamic stability, we calculate the enthalpy of formation of Li_2K with respect to elemental Li and K. It is well known that if the enthalpy of formation is negative, the compound is thermodynamically stable against decomposition into elements. As presented in Fig. 2(a), our calculations show that the $C2/m$ and $Fddd$ phases have positive formation enthalpies under pressures below 285 GPa, indicating that both phases are thermodynamically metastable below this pressure. The evolution of formation enthalpy with pressure indicates that the $C2/m$ phase transforms to the $Fddd$ one at 226 GPa, and then to the $I4/mmm$ phase at 291 GPa. The $I4/mmm$ phase finally remains stable up to at least 700 GPa. We also performed structure searches for Li-rich Li_xK ($x = 4/3$, 3/2 and 1–4) at 300 GPa, and no other compound was found to be thermodynamically stable apart from Li_2K.

From a thermodynamic point of view, the formation enthalpy of a compound is made up of two parts, i.e., the relative internal energy ΔU and the $p\Delta V$ term ($\Delta H = \Delta U + p\Delta V$). To gain deeper insights into the thermodynamic mechanism of the pressure-stabilized Li_2K, we plot the pressure-dependent ΔU and $p\Delta V$ in Figs. 2(b)–2(d) for the three phases. It is seen that the values of $p\Delta V$ are mostly negative, while ΔU is the opposite. This result reveals that the formation of Li_2K is mainly contributed by the low $p\Delta V$ that represents better atomic packing in the compound than in elemental Li and K, rather than the high ΔU that denotes strong Coulomb repulsion of Li and K atoms. This is reasonable since achieving a high packing efficiency is necessary for the stability of materials under high compression.

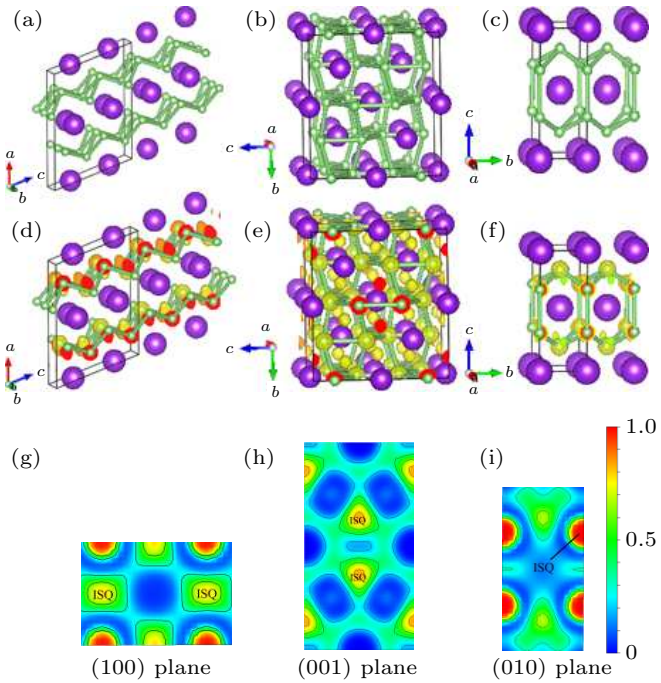


Fig. 1. Crystal structures, three-dimensional plots (isosurface value = 0.6) and two-dimensional plots of the electron localization function of (a), (d) and (g) $C2/m$-Li_2K, (b), (e), and (h) $Fddd$-Li_2K, and (c), (f) and (i) $I4/mmm$-Li_2K at 250 GPa, 290 GPa and 700 GPa, respectively. Purple and green spheres correspond to K and Li atoms, respectively.

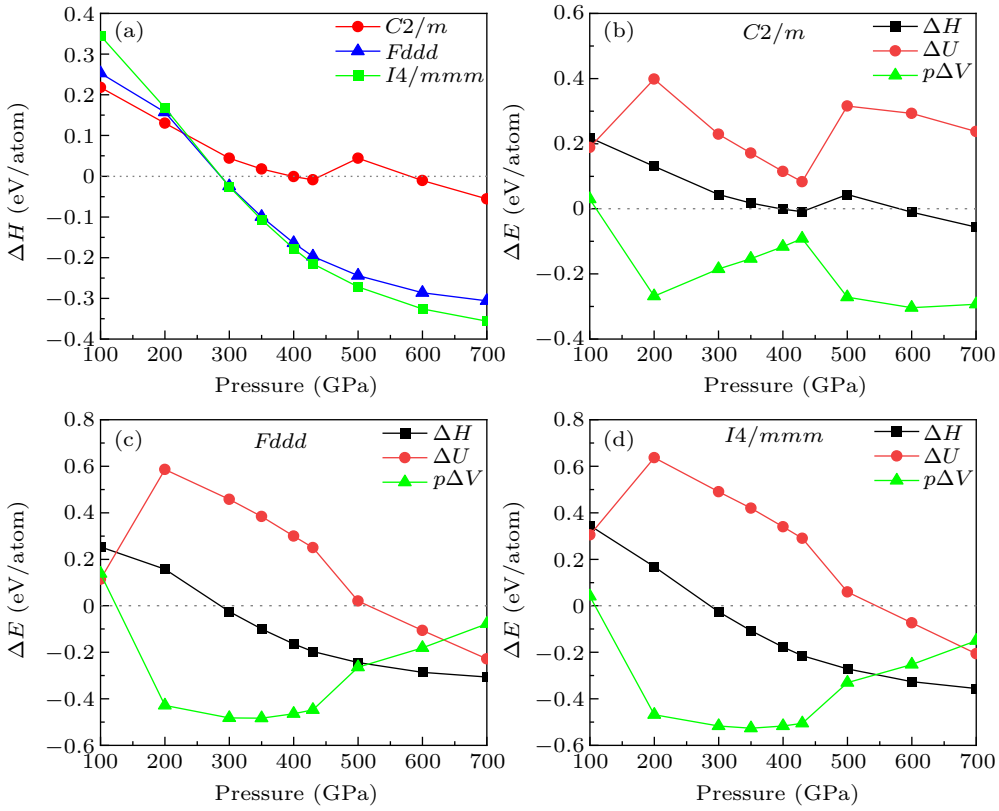


Fig. 2. Pressure dependent enthalpy of formation (a) and relative internal energy ΔU and $p\Delta V$ for (b) $C2/m$-Li_2K, (c) $Fddd$-Li_2K and (d) $I4/mmm$-Li_2K.

In order to understand the nature of chemical bonds in Li_2K, we calculate the electron localization functions (ELFs)[56] and perform Bader charge analysis.[57] for the three phases. As shown in Figs. 1(d)–1(i), all three phases exhibit the nature of a zero-dimensional electride, evidenced by the strong localization of electrons in the interstitial sites of crystals. The ELF values are less than 0.5 between all the atoms, which is typical for ionic or metallic bonding. It should be emphasized that no covalent interaction has been found here even though the Li atoms arrange in Li layers or Li cages as described above. This phenomenon indicates that the Li layers or Li cages are stabilized by compression rather than the chemical bonding itself.

According to the Bader charge analysis presented in Table 1, the Li atoms in all three phases lose electrons. Some of the lost electrons of Li transfer to the K atoms, resulting in the oxidation of K; the rest transfer to the interstitial sites, leading to the formation of an electride. The results of Bader analysis reveal ionic interactions between Li and K as well as the ISQ electrons, consistent with the ELF calculations. It is worth noting that as the pressure increases, the Bader charge of ISQ decreases, indicating that the localization of interstitial electrons is suppressed by pressure in the Li–K system. This is counterintuitive and in contrast to elemental Li where compression would generally promote the transfer of valence electrons into ISQs because the energy level of valence orbitals of atoms surpasses that of ISQs.

Table 1. Bader charge ($|e|$ per formula unit, Li_2K) of $C2/m$ Li_2K, $Fddd$ Li_2K and $I4/mmm$ Li_2K at different pressures.

Phase	Pressure (GPa)	K	Li (e/cell)	ISQ (e/cell)
$C2/m$	200	−0.77	1.23	−0.45
	250	−0.84	1.21	−0.36
$Fddd$	290	−0.83	1.24	−0.41
	300	−0.84	1.24	−0.39
$I4/mmm$	300	−0.89	1.20	−0.30
	500	−1.01	1.19	−0.18
	700	−1.06	1.18	−0.12

In Fig. 3, the total and projected electronic density of states (DOS) of $C2/m$ Li_2K at 250 GPa, $Fddd$ Li_2K at 290 GPa and $I4/mmm$ Li_2K at 700 GPa are presented. It is shown that the DOS plots of the three phases exhibit similar characteristics. All of them show a typical metallic nature evidenced by substantial DOS distributions at the Fermi level (E_F). The projected DOS reveal significant s → p and s → d charge transfer in Li and K, respectively. The states around the Fermi level are dominantly contributed by these Li 2p and K 3d orbital electrons. Particularly noteworthy is the significant contribution of s states of ISQ at the Fermi level and their strong hybridization with Li 2p orbitals. Figure 3 reveals that as pressure increases, the ISQ states at the Fermi level decrease significantly, which is consistent with the Bader charge analysis. Meanwhile the sp hybridization also weakened. It is worth noting that these sp-hybridized electronic states are anticipated to exhibit enhanced orbital multiplicity flexibility, facilitating the forma-

tion of stable Cooper pairs more efficiently than traditional Li s electrons.[42,58] Therefore, the superconductivity of Li_2K is also worth looking at (see later). These pressure-driven superconductivity mechanisms are somewhat similar to that of elemental Li, where pressure-induced transformation of s to p orbitals promotes superconductivity.[58]

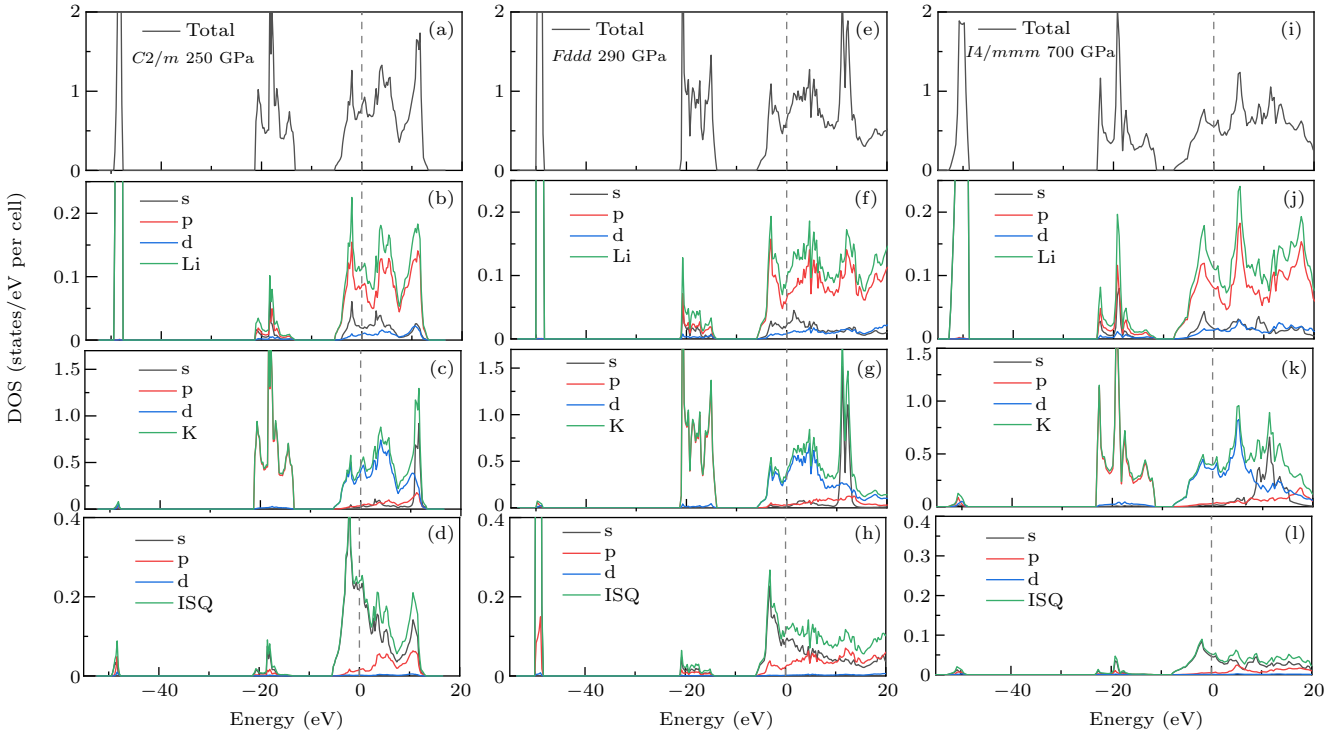


Fig. 3. The total and projected electronic density of states of (a)–(d) $C2/m$-Li_2K at 250 GPa, (e)–(h) $Fddd$-Li_2K at 290 GPa and (i)–(l) $I4/mmm$-Li_2K at 700 GPa, including the semi-core states and the valence states. The zero of energy is placed at the Fermi energy.

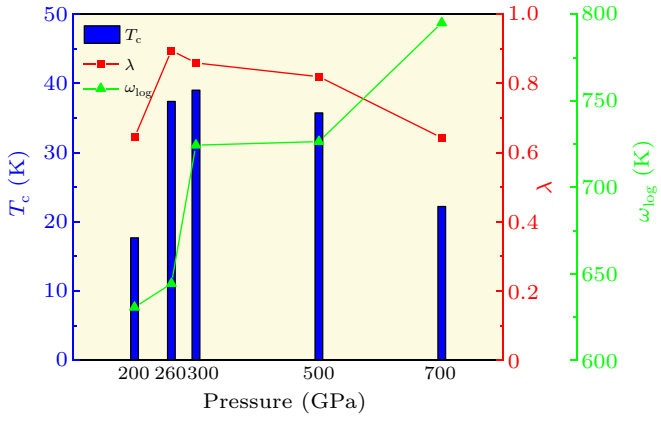


Fig. 4. The variation of T_c, λ and ω_{log} with pressure for Li_2K.

We then calculate the superconducting critical temperature (T_c) by using the Allen–Dynes-modified McMillan equation[59] $T_c = \frac{\omega_{log}}{1.2}\exp[-\frac{1.04(1+\lambda)}{\lambda-\mu^*(1+0.62\lambda)}]$, where ω_{log} is the logarithmic average frequency, λ is the e–p coupling parameter and μ^* is the Coulomb pseudopotential (here a typical value of $\mu^* = 0.1$ is used). As expected, Li_2K has strong e–p coupling and remarkable superconductivity. As illustrated in Fig. 4, the calculated T_c of Li_2K exhibits an overall proportional relationship with λ. T_c first increases from 17 K at 200 GPa to 37 K at 260 GPa and then up to 39 K at 300 GPa accompanied by the phase transition of $C2/m \rightarrow Fddd \rightarrow I4/mmm$. Above 300 GPa, T_c decreases nearly linearly to 22 K at 700 GPa. The highest value of λ is 0.9 in the $Fddd$ phase at 260 GPa. After the transition from the $Fddd$ to the $I4/mmm$ phase, λ decreases monotonously with pressure. This decrease in λ may be attributed to the decrease of ISQ and the weakened s–p hybridization, which is believed to play significant role in enhancing e–p coupling.[34,42]

In Fig. 5, we plot the frequency dependence of e–p coupling $\lambda(\omega)$ and the Eliashberg spectral function $\alpha^2F(\omega)$, in combination with the phonon density of states and phonon dispersion spectra. The phonon dispersion spectra (Figs. 5(a)–5(c)) exhibit no imaginary frequencies in the entire Brillouin zone, confirming the dynamic stability of the three structures and supporting their experimental synthesizability. In the $C2/m$ phase, as depicted in Fig. 5(d), the $\alpha^2F(\omega)$ spectrum can be distinctly divided into two components. The first component is a broad distribution spanning the frequency range 10–33 THz, which corresponds to the higher-frequency vibrational modes of Li and K atoms. The second component is a narrower distribution within the 0–10 THz range, primarily attributable to the vibration of K atoms. These two segments contribute 74% and 26%, respectively, to the overall e–p coupling λ. In the $Fddd$ and $I4/mmm$ phases (Figs. 5(e) and 5(f), the vibrational contributions from Li atoms dominate at higher frequencies, while those from K atoms prevail at lower frequencies. The frequency-dependent λ and

$\alpha^2F(\omega)$ suggest that vibrational modes across both lower and higher frequencies contribute almost equally to λ. This observation indicates that the phonons associated with both Li and K atoms play significant roles in the e–p coupling process. This mechanism stands in contrast to that of other superconductors such as Al_4H[60] and VN_2,[61] which largely depend on low-frequency modes, and Sc_4H,[62] which relies on mid–high-frequency phonons.

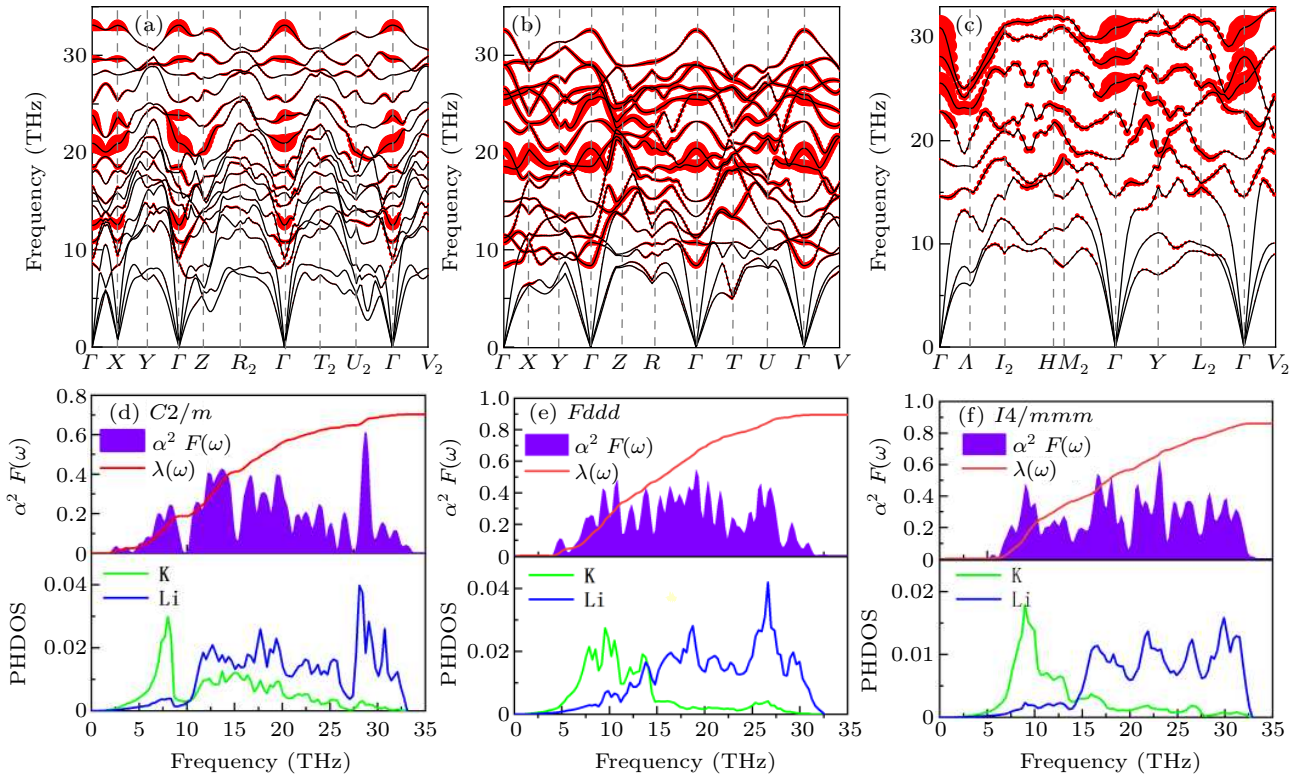


Fig. 5. Phonon dispersion spectrum, Eliashberg spectral functions $a^2F(\omega)$, electron–phonon coupling $\lambda(\omega)$ and phonon density of states (PHDOS) of (a) and (d) $C2/m$ Li_2K, (b) and (e) *Fddd* Li_2K, and (c) and (f) $I4/mmm$ Li_2K at 20 GPa, 260 GPa, and 300 GPa, respectively. Red solid circles represent the phonon linewidth with a radius proportional to the strength.

In addition, we observed pronounced phonon softening at the X point of the $C2/m$ phase, along the X–Y direction in *Fddd*, and along the I_2–I direction of the $I4/mmm$ phase, all occurring within the frequency range below 10 THz. Similarly, soft phonon modes were detected in systems such as Li_6P,[34] $Li_{10}Si$,[43] Li_6C,[42] and VN_2,[42] which are probably associated with the hybridization of orbitals near the Fermi level and thereby promote Cooper pairing and enhanced e–p coupling. At higher frequencies (10–35 THz), notably, the optical phonon modes exhibit large linewidths and significant broadening, as observed in Al_4H,[60] Li_6C[42] and Li_6P.[34] The pronounced broadening and high-weighted projections of these phonons suggest cooperative interactions among ISQ states, involving Li and K atoms, which further strengthen the e–p coupling.

4. Conclusion

In summary, we have performed a first-principles study on the phase stability, electronic and superconducting properties of Li_2K under high pressures. We uncovered three stable/metastable phases with interesting structures, including Li layers and Li cages. All the three phases exhibit typical metallic and electride natures at certain pressures. Significant s $\rightarrow$ p and s $\rightarrow$ d charge transfer has been found in Li and K atoms, respectively. An overall pressure-induced weakening of interstitial electron localization was predicted in Li_2K which is anomalous with respect to that of elemental Li and K. Owing to the hybridization of Li p and ISQ s orbital electrons and their strong coupling with the phonons of Li and K atoms, Li_2K was predicted to be a potential superconductor with its highest T_c of 39 K at 300 GPa. Our results highlight the intricate interplay between pressure, electronic structure and superconductivity in Li_2K, providing valuable insights for further investigations into novel chemical and physical properties in alkali metals or their compounds.

Acknowledgments

Project supported by the National Natural Science Foundation of China (Grant Nos. 12364003, 11804131 and 11704163), the Natural Science Foundation of Jiangxi Province of China (Grant Nos. 20252BAC240168, 20232BAB211022, and 20181BAB211007), and the Natural Science Foundation of Henan Province (Grant No. 242300421689).

References

[1] Hanfland M, Syassen K, Christensen N E and Novikov D L 2000 *Nature* **408** 174
[2] Ma Y, Oganov A R and Xie Y 2008 *Phys. Rev. B* **78** 014102
[3] McMahon M I, Nelmes R J, Schwarz U and Syassen K 2006 *Phys. Rev. B* **74** 140102
[4] Rousseau B, Xie Y, Ma Y and Bergara A 2011 *Eur. Phys. J. B* **81** 1
[5] Tsuppayakorn-Aek P, Luo W, Watcharatharapong T, Ahuja R and Bovornratanaraks T 2018 *Sci. Rep.* **8** 5278
[6] Woolman G, Naden Robinson V, Marqués M, Loa I, Ackland G J and Hermann A 2018 *Phys. Rev. Mater.* **2**
[7] Yao Y, Tse J S and Klug D D 2009 *Phys. Rev. Lett.* **102** 115503
[8] Wang X, Wang Z, Gao P, Zhang C, Lv J, Wang H, Liu H, Wang Y and Ma Y 2023 *Nat. Commun.* **14** 2924
[9] Wang B, Hilleke K P, Wang X, Polsin D N and Zurek E 2023 *Phys. Rev. B* **107** 184101
[10] Racioppi S, Storm C V, McMahon M I and Zurek E 2023 *Angew. Chem.* **135** e202310802
[11] Miao M S, Hoffmann R, Botana J, Naumov I I and Hemley R J 2017 *Angew. Chem.* **129** 992
[12] Li Y, Wang Y, Pickard C J, Needs R J, Wang Y and Ma Y 2015 *Phys. Rev. Lett.* **114** 125501
[13] Matsuoka T, Sakata M, Nakamoto Y, Takahama K, Ichimaru K, Mukai K, Ohta K, Hirao N, Ohishi Y and Shimizu K 2014 *Phys. Rev. B* **89** 144103
[14] Lv J, Wang Y, Zhu L and Ma Y 2011 *Phys. Rev. Lett.* **106** 015503
[15] Ma Y, Eremets M, Oganov A R, Xie Y, Trojan I, Medvedev S, Lyakhov A O, Valle M and Prakapenka V 2009 *Nature* **458** 182
[16] Schaeffer A M, Temple S R, Bishop J K and Deemyad S 2015 *Proc. Natl. Acad. Sci. USA* **112** 60
[17] Shimizu K, Ishikawa H, Takao D, Yagi T and Amaya K 2002 *Nature* **419** 597
[18] Struzhkin V V, Eremets M I, Gan W, Mao H K and Hemley R J 2002 *Science* **298** 1213
[19] Huang H M, Zhu Q, Blatov V A, Oganov A R, Wei X, Jiang P and Li Y L 2023 *Nano Lett.* **23** 5012
[20] Yang L, Qu X, Zhong X, Wang D, Chen Y, Lang J, Liu C, Sun B and Yang J 2021 *Comp. Mater. Sci.* **200** 110818
[21] Frost M, McBride E E, Schörner M, Redmer R and Glenzer S H 2020 *Phys. Rev. B* **101** 224108
[22] Yang L, Qu X, Zhong X, Wang D, Chen Y, Yang J, Lv J and Liu H 2019 *J. Phys. Chem. Lett.* **10** 3006
[23] Dong X, Oganov A R, Goncharov A F, Stavrou E, Lobanov S, Saleh G, Qian G R, Zhu Q, Gatti C, Deringer V L, Dronskowski R, Zhou X F, Prakapenka V B, Konópkova Z, Popov I A, Boldyrev A I and Wang H T 2017 *Nat. Chem.* **9** 440
[24] Chen Y M, Geng H Y, Yan X Z, Wang Z W, Chen X R and Wu Q 2017 *Chin. Phys. B* **26** 056102
[25] Chen Y, Chen X, Wu Q, Geng H, Yan X, Wang Y and Wang Z 2016 *J. Phys. D: Appl. Phys.* **49** 355305
[26] Botana J and Miao M S 2014 *Nat. Commun.* **5** 4861
[27] Zhang X and Zunger A 2010 *Phys. Rev. Lett.* **104** 245501
[28] Xie Y, Oganov A R and Ma Y 2010 *Phys. Rev. Lett.* **104** 177005
[29] Desgreniers S, John S T, Matsuoka T, Ohishi Y and Justin J T 2015 *Sci. Adv.* **1** e1500669
[30] Chen Y, Yan X, Geng H, Sheng X, Zhang L, Wang H, Li J, Cao Y and Pan X 2021 *Inorg. Chem.* **60** 124
[31] Pereira Z S, Faccin G M and da Silva E Z 2021 *J. Phys. Chem. C* **125** 8899
[32] Wang Q, Cui W, Gao K, Chen J, Gu T, Liu M, Hao J, Shi J and Li Y 2022 *Phys. Rev. B* **106** 054519
[33] Xu W, Wang Q, Zeng Q, Li X, Shi J, Hao J, Cui W and Li Y 2025 *Comput. Mater. Today* **5** 100017
[34] Liu Z, Duan D, Zhuang Q and Cui T 2023 *Phys. Rev. B* **108** L100507
[35] Novoselov D Y, Korotin D M, Shorikov A O, Anisimov V I and Oganov A R 2024 *Phys. Chem. Chem. Phys.* **26** 17854
[36] Zhang X, Yao Y, Ding S, Bergara A, Li F, Liu Y, Zhou X F and Yang G 2023 *Phys. Rev. B* **107** L100501
[37] Guo Z, Bergara A, Zhang X, Li X, Ding S and Yang G 2024 *Phys. Rev. B* **109** 134505
[38] Wang X, Wang Y, Wang J, Pan S, Lu Q, Wang H T, Xing D and Sun J 2022 *Phys. Rev. Lett.* **129** 246403
[39] Zhao Y, Bergara A, Zhang X, Li F, Liu Y and Yang G 2023 *Phys. Rev. B* **108** 104505
[40] Wang Q, Wei J, Zhong T, Sun J, Gao B, Zhu L, Liu H and Zhang S 2024 *Phys. Rev. B* **110** 144523
[41] Zhang X, An T and Yang G 2025 *Comput. Mater. Today* **5** 100020
[42] Liu Z, Zhuang Q, Tian F, Duan D, Song H, Zhang Z, Li F, Li H, Li D and Cui T 2021 *Phys. Rev. Lett.* **127** 157002
[43] Wang Q, Cui W, Xu W, Gao K, Hao J, Shi J, Liu H and Li Y 2024 *Phys. Rev. B* **110** 134114
[44] Gao B, Gao P, Lu S, Lv J, Wang Y and Ma Y 2019 *Sci. Bull.* **64** 301
[45] Wang H, Wang Y C, Lv J, Li Q, Zhang L J and Ma Y M 2016 *Comp. Mater. Sci.* **112** 406
[46] Wang Y, Lv J, Zhu L, Lu S, Yin K, Li Q, Wang H, Zhang L and Ma Y 2015 *J. Phys. Condens. Matter* **27** 203203
[47] Wang Y C, Lv J, Zhu L and Ma Y M 2012 *Comput. Phys. Commun.* **183** 2063
[48] Kresse G and Furthmüller J 1996 *Phys. Rev. B* **54** 11169
[49] Miao M S, Zhang M L, Van Doren V E, Ladik J J and Mintmire J W 2000 *J. Phys. Chem. A* **104** 6809
[50] Toulouse J and Savin A 2006 *J. Mol. Struct.-Theochem* **762** 147
[51] Blöchl P E 1994 *Phys. Rev. B* **50** 17953
[52] Giannozzi P, Baroni S, Bonini N, *et al.* 2009 *J. Phys. Condens. Matter* **21** 395502
[53] Lv J, Wang Y, Zhu L and Ma Y 2011 *Phys. Rev. Lett.* **106** 015503
[54] Pickard C J and Needs R J 2009 *Phys. Rev. Lett.* **102** 146401
[55] Lundegaard L F, Marqués M, Stinton G, Ackland G J, Nelmes R J and McMahon M I 2009 *Phys. Rev. B* **80** 020101
[56] Becke A D and Edgecombe K E 1990 *J. Chem. Phys.* **92** 5397
[57] Bader R F 1990 *Atoms in Molecules* (Wiley Online Library)
[58] Christensen N and Novikov D 2001 *Phys. Rev. Lett.* **86** 1861
[59] Allen P B and Dynes R C 1975 *Phys. Rev. B* **12** 905
[60] He Y, Lu J, Wang X and Shi J J 2023 *Phys. Rev. B* **108** 054515
[61] Yin Y, Chen F, Hu G, Zhao X, Yuan X and Ren J 2025 *Phys. Rev. B* **111** 064519
[62] Guan Z, Cui T and Li D 2025 *Phys. Rev. B* **111** 014516